13th World Conference on Earthquake Engineering
Vancouver, B.C., Canada
August 1-6, 2004
Paper No. 20

A NEW PROPOSAL FOR LIQUEFACTION POTENTIAL BASED ON ENERGY BALANCE METHOD

Shuichi SHIMOMURA [1], Noriaki SAKO [2], Toshio ADACHI [3]

SUMMARY

In this study, a new method for the evaluation of liquefaction potential based on energy balance is proposed using pseudo-dynamic tests. This method has been developed to evaluate the liquefaction potential and dynamic property of surface layers by using commonly used parameters such as initial shear modulus, reference strain and liquefaction resistance. In order to verify the proposed method, a simulation analysis was conducted on the soil of two different artificial islands, Kobe Port Island and Rokko Island, where the liquefaction damages were observed in the 1995 Hyogoken Nambu Earthquake. Though the two islands are closely located, significant different liquefaction damages were observed. Although it is difficult to represent such different damage patterns by the present simple method used in Japan, however, the proposed method can effectively evaluate the actual damage by in consideration of the difference of the stiffness of clay layer underlying the reclaimed ground.

INTRODUCTION

As a simplified procedure for evaluating liquefaction potential, the F_l method [1] is often used in Japan. This method compares liquefaction resistance ratio τ_l/σ_0' with shear stress ratio τ_d/σ_0' that might have developed in the field during the earthquake, and liquefaction potential is evaluated ($\tau_l/\sigma_0' \leq \tau_d/\sigma_0'$: It is evaluated that the liquefaction potential is high). With this method the shear stress ratio τ_d/σ_0' is defined by Eq.(1).

$$\tau_d \Big/ \sigma_0' = \frac{\alpha_{\max}}{g}\frac{\sigma_0'}{\sigma_0}\gamma_d \cdot \gamma_n \qquad (1)$$

where, α_{max}: the maximum acceleration at ground surface, g: the gravity acceleration, σ_0': the initial effective vertical stress, σ_0: the total vertical stress. The parameters γ_d and γ_n are correction factors in terms of depth, z in meters, and earthquake magnitude, M, respectively, as follows

[1] Research Engineer, Technical Research Institute, Kajima Co., Japan
[2] Graduate Student, Dept. of Architecture, College of Science & Technology, Nihon Univ., Japan
[3] Professor, Dept. of Architecture, College of Science & Technology, Nihon Univ., Japan

$$\gamma_d = 1 - 0.015z \tag{2}$$

$$\gamma_n = 0.1 \cdot (M - 1) \tag{3}$$

The reduction coefficient γ_d is strongly dependent on the predominant period of the input earthquake motion and the natural period of the ground [2], however the shear stress ratio does not take into account the effect of the predominant period of the input earthquake motion and the natural period of the ground. In particular, Kazama [3] showed that it is difficult to explain the level of damage from the shear stress when the frequency characteristics of the input earthquake motion is ignored. Moreover, the influence of layer constitution is not considered in this method because the liquefaction potential of each layer is evaluated independently. Yamaguchi [4] reported that the different degrees of damage between two artificial islands, Kobe Port Island and Rokko Island, was due to the different stiffnesses due to the degree of consolidation of the clay layer underlying the reclaimed ground.

Some studies on liquefaction potential based on an energy concept have been reported. Igarashi [5] proposed a method based on the concept of dislocation energy. Kazama [6] proposed an evaluation procedure based on the relationship between cumulative dissipation energy, modulus reduction rate and pore water pressure. However, these methods require many parameters associated with analytical procedures, which makes them difficult to apply in practice.

This paper proposes a new method for determining liquefaction potential based on "energy balance" derived from pseudo-dynamic tests. This method has been developed to evaluate the liquefaction potential and dynamic properties of surface layers by using commonly used parameters such as initial shear modulus, reference strain and liquefaction resistance. In addition, the method considers the influence of the predominant period of the input earthquake motion, the natural period of the ground and the layer constitution.

OUTLINE OF PROPOSED EVALUATION PROCEDURE FOR LIQUEFACTION

An energy balance formula is obtained from the equation of motion where each term is multiplied by velocity vector and integrates to an arbitrary time.

$$\int_0^t \{\dot{x}\}^T [M]\{\ddot{x}\}dt + \int_0^t \{\dot{x}\}^T [C]\{\dot{x}\}dt + \int_0^t \{\dot{x}\}^T \{R\}dt = -\int_0^t \ddot{y}\{\dot{x}\}^T [M]\{i\}dt \tag{4}$$

where, [M]: mass matrix, [C]: damping matrix, {R}: restoring force vector, $\{\ddot{x}\}$: relative acceleration vector, $\{\dot{x}\}$: relative velocity vector, $\ddot{y}$: input acceleration and {i}: unit vector.

Eq. (4) can be expressed as

$$W_e + W_h + W_p = E \tag{5}$$

where, W_e: elastic vibration energy (the sum of elastic strain energy and kinetic energy), W_h : dissipation energy by viscous damping, W_p: cumulative plastic strain energy, and E: input energy. Eq. (4) is an energy balance formula per unit cross sectional area.

Akiyama [7] developed the concept of energy input and proposed seismic design methods based on energy balance. The concept is applied to the liquefaction potential of the ground in this study. Liquefaction potential based on the energy balance method is based on the following three items:
1) The total input energy in the surface layers above the engineering bedrock.
2) The energy distribution ratio of each layer.
3) The energy absorption potential (cumulative plastic strain energy).

PSEUDO-DYNAMIC TESTING METHOD

Pseudo-dynamic tests were conducted to simulate non-linear behavior of saturated sand, and to verify the validity of the proposed method. The pseudo-dynamic testing method for a geotechnical system comprises a hybrid experiment combining earthquake response analysis with laboratory dynamic soil tests using a computer on-line data processing system. This method can represent the stress-strain relationship without using a mathematical model.

One layer or two layers were modeled as a lumped mass model with a one or two degrees of freedom, as illustrated in Fig.1. The tests of one-layer model were conducted to examine input energy, and the tests of two-layer model were conducted to examine the energy distribution ratio of each layer and the energy absorption potential. The test method was described in detail in Kusakabe et al. [8] and Adachi et al. [9]. The test conditions are shown in Table 1 and Table 2. The apparatuses for the pseudo-dynamic test were hollow torsional shear test equipment. A twin-type apparatus was used in the test of two-layer model. The test samples were Toyoura sand which is clean fine sand with a mean grain size between 0.1 to 0.2mm. The initial confining stress was equivalent to an initial effective vertical stress of an intermediate point in each layer. In the one-layer model, relative density was around at 60%, and four kinds of actual earthquake waves with different predominant periods were used for the input motion. In the two-layer model, the relative density of the upper layer was fixed around at 65% and three combinations of relative density (50%, 65% and 80%) were fixed in the lower layer, and six kinds of actual earthquake waves with different predominant periods were used for the input motion. In addition cyclic undrained shear tests were conducted to examine influence of stress history for cumulative strain energy. The test condition is shown in Table 3. The test samples were Toyoura sand, the apparatus is hollow torsional shear test equipment and relative density was around at 50% and 80%.

It was necessary to continuously measure from small to large strain levels in Pseudo-dynamic test, but we could not measure over 2.5% shear strain of double amplitude. Therefore, in this study, initial liquefaction was defined as that when the pore water pressure ratio increased to 1.0.

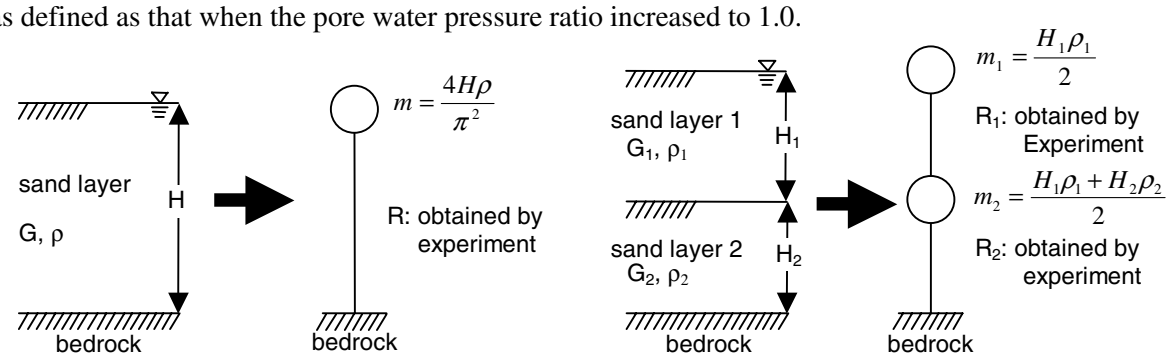

$$m\ddot{x} + c\dot{x} + R = -m\ddot{y}$$

$$\begin{bmatrix} m_1 & 0 \\ 0 & m_2 \end{bmatrix}\begin{Bmatrix} \ddot{x}_1 \\ \ddot{x}_2 \end{Bmatrix} + \begin{bmatrix} c_1 & -c_1 \\ -c_1 & c_1 + c_2 \end{bmatrix}\begin{Bmatrix} \dot{x}_1 \\ \dot{x}_2 \end{Bmatrix} + \begin{Bmatrix} R_1 \\ R_2 - R_1 \end{Bmatrix} = -\begin{bmatrix} m_1 & 0 \\ 0 & m_2 \end{bmatrix}\begin{Bmatrix} \ddot{y} \\ \ddot{y} \end{Bmatrix}$$

c: damping coefficient, m: mass, R: restoring force
(the viscous damping is negligible, since the predominance damping is hysteretic in sand)

Fig.1 Lumped mass model

Table.1 Test condition on one degree of freedom

Case No.	Ground model						Input motion		
	Relative density (%)	Initial confining pressure (kPa)	Initial shear modulus (MPa)	Thickness (m)	Wet density (kN/m^3)	Initial natural period (sec)	Name	Maximum input acceleration (cm/s^2)	Predominant period (sec)
case1	57-60	28	43-45	5	19.2-19.4	0.13-0.23	El-Centro_1940 (NS)	100-275	0.68
case2	56-63	32	43-50	6				100-250	
case3	55-62	41	54-55	8				100-250	
case4	62	49	57	10				175	
case5	58	29	46	6		0.15-0.23	Taft (EW)	130	0.44
case6	63-65	49	55-59	10				100-175	
case7	62-65	49	54-59	10		0.23-0.24	Hachinohe (EW)	70-150	1.10
case8	56-61	49	59-61	10		0.22-0.23	Kobe (NS)	150-200	0.71

Table.2 Test condition on two degree of freedom

Case No.	Ground model							Input motion		
	Layer	Relative density (%)	Initial confining pressure (kPa)	Initial shear modulus (MPa)	Thickness (m)	Wet density (kN/m^3)	Initial natural period (sec)	Name	Maximum input acceleration (cm/s^2)	Predominant period (sec)
case9	Upper	66	23	40	5	19.1-19.8	0.23-0.24	Kushiro (EW)	250	0.18
	Lower	81	74	79	5					
case10	Upper	67	25	45	5				250	
	Lower	63	74	73	5					
case11	Upper	68	25	43	5				250	
	Lower	48	74	63	5					
case12	Upper	63	26	40	5			Taft (EW)	300	0.44
	Lower	80	74	84	5					
case13	Upper	63	25	45	5				300	
	Lower	67	74	74	5					
case14	Upper	67	23	39	5				300	
	Lower	50	71	66	5					
case15	Upper	66	25	44	5			Kobe Port Island (NS)	400	1.8
	Lower	84	74	81	5					
case16	Upper	63	23	41	5				400	
	Lower	63	74	69	5					
case17	Upper	68	25	44	5				300	
	Lower	55	70	62	5					

Table.3 Cyclic undrained shear test condition

Case No.	Relative density (%)	Initial confining pressure (kPa)	Initial shear modulus (MPa)	Wet density (kN/m^3)	Cyclic stress ratio
case18	48	98	88	19.1-19.7	0.17
case19	50		82		0.23
case20	52		86		0.20
case21	77		91		0.32
case22	79		94		0.27
case23	81		95		0.23

ENERGY CHARACTERISTICS OF GROUND DUE TO EARTHQUAKE MOTION

Energy absorption potential

When time histories of shear stress and shear strain are given, the cumulative plastic strain energy Wp is calculated as follows

$$W_p = \oint \tau(\gamma) d\gamma = \int_0^t \tau(\gamma)\dot{\gamma}(t) dt \qquad (6)$$

An example of the relationship between pore water pressure ratio $\Delta u/\sigma_c'$ and cumulative plastic strain energy normalized by initial effective confining stress W_p/σ_c' was shown in Fig.2. Circles in Fig.2 show the points where shear stress τ was zero after the buildup of pore water pressure. From Fig.2, we picked up the several circles with each specimen from the test results of the two-layer model and plotted those in Fig.3. There is a strong correlation between the pore water pressure and the cumulative strain energy for each relative density. But this relationship is not influenced by the stress history. The upper limitation of cumulative plastic strain energy is as high as relative density when the pore water pressure is built up to 1.0. In other words, the upper limitation of the plastic strain energy that can accumulate in sand is uniquely determined from both the soil material and initial effective confining stress, and is regarded as energy absorption potential at the initial liquefaction.

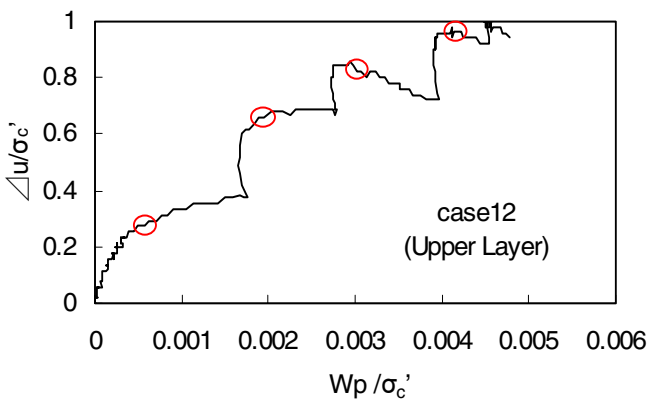

Fig.2 An example of relationship between pore water pressure ratio and cumulative plastic energy

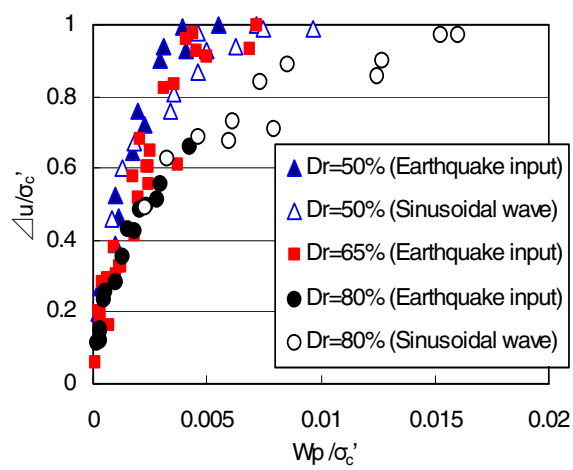

Fig.3 Relationship between pore water pressure ratio and cumulative plastic energy

Estimation of input energy

(1) Energy spectrum

In the earthquake-resistant design for buildings, the energy spectrum is used to evaluate the input energy to a building. The energy spectrum is given as the relationship between the velocity V_E converted from the total input energy E and natural period of the building T. The total energy is calculated from the one degree of freedom system.

$$V_E(T) = \sqrt{2E/M} \qquad (7)$$

where E: input energy, M: mass of the building.

Independent of the earthquake wave type, the energy increases as the natural period of the equivalent elastic model system lengthens, indicating a peak at a certain period, and descends gradually above the long period area. Akiyama [7] proposed an energy spectrum form as a general elastic system, as shown in Fig.4. As the ground motion above the engineering bedrock is usually affected by the primary mode during an earthquake, the input energy was estimated from the primary natural period. Because the damping ratio of the soil is generally higher than that of the superstructure, the energy spectra of which the damping ratio h equals 0.2 were adopted for the energy input.

(2) Effective period

The ground liquefaction under cyclic shear loading causes shear modulus reduction and extends the effective natural period of the ground. Therefore the input energy may be underestimated if the energy is evaluated from the initial natural period. A concept of effective period T_1 was thus introduced to estimate the energy spectrum of an elasto-plastic system from that of elastic system.

$$T_1 = (\kappa + 1) \cdot T_0 \qquad (8)$$

The parameter κ was estimated from Eqs.(9)-(11), focusing on the intensity of input earthquake motion and the shear strength of the ground, because it was necessary to take the modulus reduction into consideration.

$$\kappa = c \cdot \sqrt{\overline{W_i} / \tau_{\max}} \qquad (9)$$

$$\tau_{\max} = G_0 \cdot \gamma_{0.5} \qquad (10)$$

$$\overline{W_i} = \frac{M \overline{V_E}^2}{2H} \qquad (11)$$

where, τ_{max}: the shear strength, G_0: the initial shear modulus, $\gamma_{0.5}$: the reference strain, $\overline{W_i}$: the intensity of the input earthquake motion, $\overline{V_E}$: mean of the converted velocity, H: thickness of the surface layer above the engineering bedrock, and c: the constant indicated in Fig.5.

The parameter $\overline{V_E}$ was the mean value of the input energy between the initial natural period to 2.5 sec referring to spectrum intensity defined by Housner. The effective period was calculated from the relationship between the energy spectrum obtained from the test results and the energy spectrum of the input earthquake motions for the test. The correlation of T_1/T_0 and $\sqrt{\overline{W_i}/\tau_{\max}}$ is summarized in Fig.5.

(3) Estimation of input energy

The input energy calculated using κ in Fig.5 was compared with that directly obtained from the test results. This comparison is shown in Fig.6. Fig.6 also displays the results from the two-layer model test (the shear strength was calculated by considering the thickness of each layer). If the calculated T_1 is over T_G in Fig.4, the input energy is evaluated as the peak value V_E(max). It is found in Fig.6 that the input energy is estimated accurately when considering the effective period, although the input earthquake motion and the natural period of the ground are different.

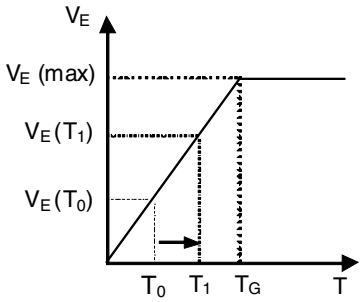

Fig.4 A general form of energy spectrum

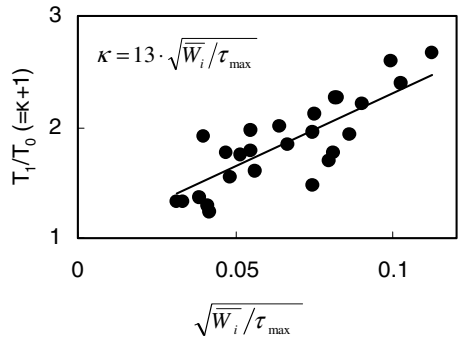

Fig.5 Estimation of effective period

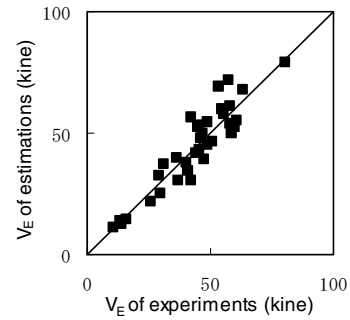

Fig.6 Comparison of V_E between estimations and experiments

Energy distribution to each layer

(1) Relationship between cumulative plastic strain energy and input energy

Fig.7(a)-(d) represents an example of the time histories of elastic vibration energy, cumulative plastic strain energy, input energy, and the ratio of cumulative plastic strain energy to the input energy, respectively. From Fig.7(a), it is found that the elastic vibration energy is varied and radiated hour by hour, and the amount of that is only a few percent of the whole input energy. Therefore, it is approximately recognized that the cumulative plastic strain energy is equal to the input energy. The ratio W_p/E showed 1.0 because the viscous damping was assumed to be zero, so it will be necessary to examine the energy absorption by viscous damping. The evaluation method for liquefaction potential developed in this study assumes that all of the input energy is consumed by plastic deformation of the ground (this assumption is on the safe side for liquefaction potential).

(2) Distribution ratio of input energy

An example of the time history of the distribution ratio of input energy is shown in Fig.8. The energy distribution ratio can be recognized to be almost constant after five seconds, where it begins to build up pore water pressure. Fig.9 shows the energy distribution ratio for the lower layer (relative density of the upper layer is approximately 65%). Thus, the characteristics of input earthquake motion may affect the energy distribution.

(3) Estimation of energy distribution ratio

From the above mentioned (1) and (2), it can be considered that the energy distribution to each layer is represented by the ratio of cumulative plastic strain energy at the strain order where pore water pressure begins to increase (strain order is 10^{-3} – this order has the limitation that it is reliable for the test results of deformation properties under cyclic load). Thus, in the proposed method, the energy distribution is estimated according to the following procedure (refer to Fig.10).

A) Calculate primary mode of surface layer above the engineering bedrock.
B) Determine the free surface displacement using acceleration response spectrum and calculate shear strain γ_i of each layer.
C) Determine shear modulus and hysteresis damping of each layer from γ_i based on strain-dependent curves (G/G_0-γ, h-γ) and update primary natural period.
D) Iterative calculation of the above procedure A)-C) until relative errors of both G_i and γ_i are become five percent or less or γ_i of one of layers reached to 10^{-3} order.

A hysteresis damping ratio was determined as follows

$$h_i = \frac{1}{4\pi}\frac{\Delta W_i}{W_i} \tag{12}$$

further,

$$W_i = G_i \gamma_i^{\ 2} / 2 \tag{13}$$

$$\Delta W_{Li} = \Delta W_i \cdot H_i = 2\pi \cdot h_i \cdot G_i \cdot \gamma_i^{\ 2} \cdot H_i \tag{14}$$

The energy distribution of each layer is estimated from

$$D_i = \frac{\Delta W_{Li}}{\sum \Delta W_{Li}} \tag{15}$$

where D_i is the energy distribution ratio of i-th layer.

Fig.11 shows the estimation results of the distribution ratio of the input energy calculated from Eq.(15). It is found that the distribution ratio was accurately estimated considering the modulus reduction by the iterative calculation.

FACTOR OF SAFETY AGAINST LIQUEFACTION OF PROPOSED METHOD

The factor of safety against liquefaction of the proposed method of i-th layer is evaluated as follows

$$F_L(E)_i = W_{Ri} / W_{Li} \tag{16}$$

$F_L(E)_i > 1.0$: Liquefaction potential is low,

$F_L(E)_i \leq 1.0$: Liquefaction potential is high,

where, $F_L(E)_i$: the factor of safety against liquefaction based on energy balance of i-th layer, W_{Ri}: the energy absorption potential of i-th layer (cumulative plastic strain energy when the pore water pressure ratio increases to 1.0 or the amplitude of the shear strain generates several per cent) and W_{Li}: the input energy distributed to i-th layer. Then W_{Li} is calculated as follows

$$W_{Li} = \frac{D_i \cdot W}{\sigma'_{ci}} \tag{17}$$

$$W = \frac{M \cdot V_E^{\ 2}}{2H} \tag{18}$$

where, W_{Li}: the distributed energy of i-th layer, σ_{ci}': the initial confining stress of i-th layer, D_i: the distribution ratio of i-th layer, M: the total mass of the surface layer above the engineering bedrock, V_E: the converted velocity given by the energy spectrum and the effective period, H: the thickness of the surface layer above the engineering bedrock.

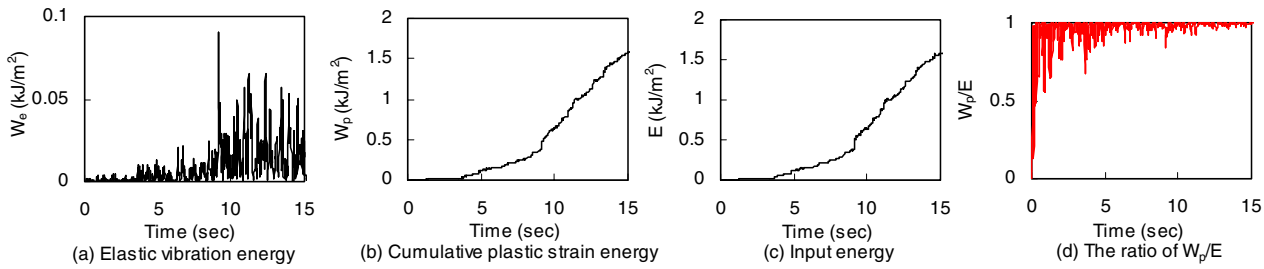

Fig.7 Time histories of energy balance (case10)

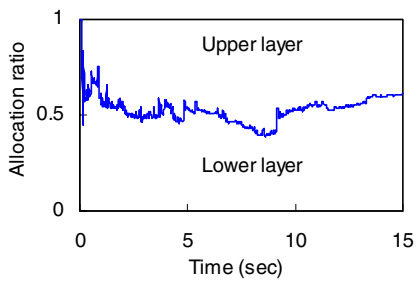

Fig.8 Time histories of distribution ratio of energy input (case10)

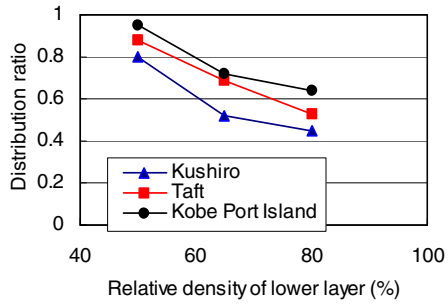

Fig.9 Effect of earthquake wave on distribution ratio

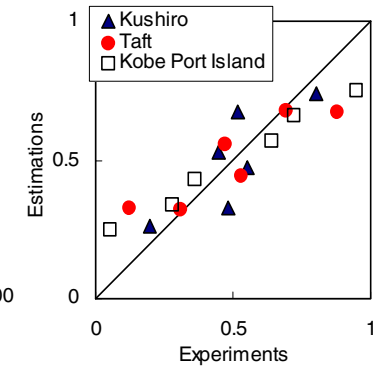

Fig.11 Comparison of distribution Ratio between estimations and experiments

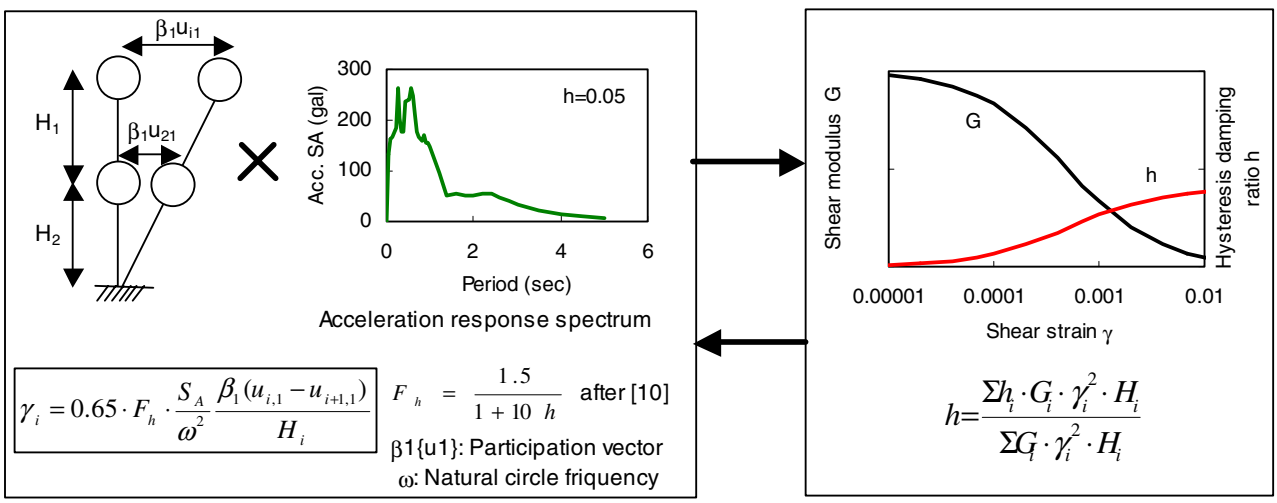

Fig.10 A procedure of iterative calculation

APPLICATION IN ACTUAL SOIL

To demonstrate the proposed factor $F_L(E)$, a simulation analysis was conducted on actual soil condition of two different artificial islands, Kobe Port Island and Rokko Island, where liquefaction damage was observed in the 1995 Hyogoken Nambu Earthquake. Although the two islands are closely located, significantly different liquefaction damage was observed. Some studies (Tanaka et al. [11]; Yamaguchi [4]) indicated that the different stiffnesses due to the degree of consolidation of the underlying clay layer

affected the seismic behavior of the reclaimed ground. In addition, a simulation analysis by the present simplified method F_l was conducted for comparison with the analysis results by the proposed method. With the present simplified method, liquefaction resistance ratio τ_l/σ_0' was referred to study [4].

Parameters for analysis

(1) Soil boring log: Soil profile, shear wave velocity, reference strain and density were decided on the basis of the Kobe City Report [12] and Yamaguchi [4]. The shear wave velocity and reference strain of the alluvial clay layer underlying Rokko Island were assumed to be those for unconsolidated clay, and these were different from those of the alluvial clay layer underlying Kobe Port Island where consolidation had been completed.

(2) Energy absorption potential: The energy absorption potential was examined from the test results of cyclic undrained triaxial tests on the undisturbed weathered granite fill (locally called Masado) and alluvial clay provided by Akihiko Uchida [13]. Fig.12 shows an example of the stress-strain relationship of the Masado and alluvial clay. It is found that the axial strain of Masado reaches approximately 8% at thirty-fourth cycle as shown in Fig.12. On the other hand, the axial strain of the alluvial clay is still 1% at 200th cycle despite the same condition of the cyclic stress ratio for Masado. The relationship between the normalized cumulative plastic strain energy and axial strain is shown in Fig.13. When the pore water pressure ratio increased to over 0.95, the normalized cumulative plastic strain energy of Masado was about 0.012. This value was equivalent to that of relative density 65%-80% of Toyoura sand, and this tendency corresponds to the study by Hatanaka et al. [13] which showed that the liquefaction resistance of Masado was nearly equal to that of relative density 70% of Toyoura sand. It is remarkable that the axial strain of the alluvial clay was only 0.5%, although the clay absorbed ten times amount of energy of Masado. Furthermore, even if more energy is absorbed, large deformation may not occur. That is, clay is a material of which energy absorption potential is very high compared with the sand or gravel.

(3) Input earthquake motion: An array record observed at Kobe Port Island (GL-32m) was used for the input motion of the simulation analysis by the $F_L(E)$ method. Energy spectrum is shown in Fig.14. When the effective period T_1 was beyond T_G (the period at the peak value of energy spectrum) at both Kobe Port Island and Rokko Island, the peak value of the input energy was used for the calculation. This input energy was 17.5kJ/m^2. The maximum acceleration at the ground surface used for the F_l method was set at 340 gal considering the maximum acceleration of the vertical array record at the free surface.

The ground model used and the simulation analysis results for the liquefaction potential are summarized in Table 4. As the liquefaction potential of each layer is evaluated independently by the F_l method, the results of both ground model were the same as when the liquefaction potential is high. However, the results of both ground model by the proposed method $F_L(E)$ were different from those considering the effect of layer constitution. This makes it difficult to represent the actual liquefaction damage at Rokko Island by the present simplified method. However, the proposed method can effectively evaluate the actual damage by introducing the difference in the stiffness of the clay layer underlying the reclaimed ground.

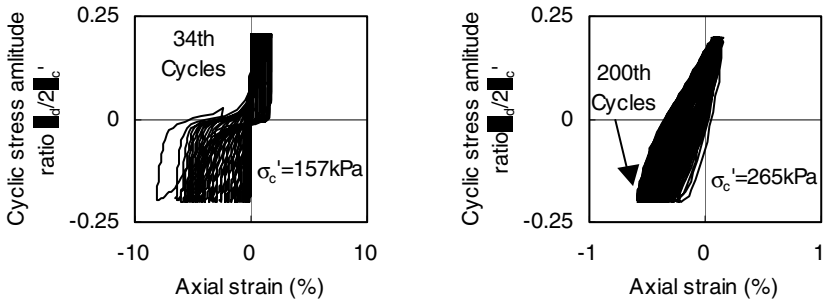

(a) Masado (b) Alluvial clay

Fig.12 Stress-strain relationship

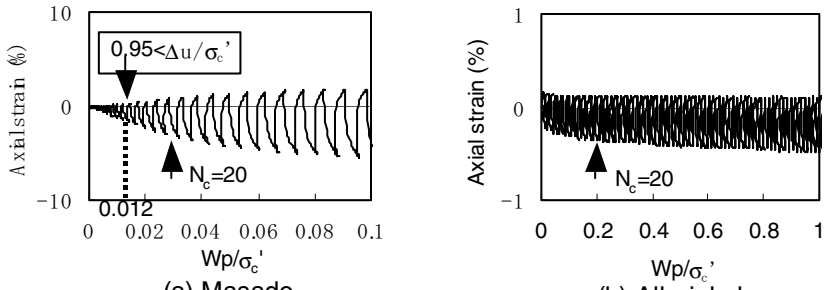

(a) Masado (b) Alluvial clay

Fig.13 Relationship between axial strain and energy absorption potential

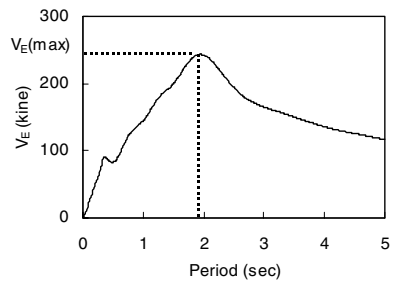

Fig.14 Energy spectrum

Table.4 Ground model and results of liquefaction potential

Soil profile		H (m)	ρ (t/m³)	R	Kobe Port Island Vs (m/s)	$\gamma_{0.5}$ ($\times10^{-3}$)	T_0 (s)	E (kJ/m²)	D	Actual damage	F_l	$F_L(E)$	Rokko Island Vs (m/s)	$\gamma_{0.5}$ ($\times10^{-3}$)	T_0 (s)	E (kJ/m²)	D	Actual damage	F_l	$F_L(E)$
Reclaimed Layer (Masado)		4.0	1.7	-	170	0.53	0.64	17.5	0.01	-	-	-	170	0.53	0.74	17.5	0	-	-	-
		5.0	2.0	0.15	210				0.15	×	×	×	210				0.005	○	×	○
		5.0		0.22						×	×	×						○	×	○
		3.4		0.17						×	×	×						○	×	○
Alluvial clay		10.8	1.6	-	**180**	**1.48**			0.74	-	-	-	**100**	**0.53**			0.99	-	-	-
Diluvial gravel		3.8	2.0	-	250	0.79			0.10				250	0.40			0.004			
engineering bedrock		-	2.0	-	310	-	-	-	-	-	-	-	310	-	-	-	-	-	-	-

H: Thickness, ρ: Density, R: Liquefaction resistance, V_S: Shear wave velocity,
$\gamma_{0.5}$: Reference strain, T_0: Initial natural period, E: Input energy, D: Distribution ratio
○ : non liquefaction, × : liquefaction

CONCLUSIONS

A new method for evaluating liquefaction potential based on energy balance is proposed. This method has the following significant features.

1) It has been developed to evaluate the liquefaction potential using commonly used parameters such as the initial shear modulus, the reference strain and the liquefaction resistance for the dynamic properties of surface layers.
2) The influence of the predominant period of the input earthquake motion, the natural period of the ground and the layer constitution are taken into consideration, and it is possible to calculate the value using a spreadsheet software.

In application to actual soil where liquefaction damage was observed, the proposed method can represent actual damage, which cannot be represented by the present simplified method F_l.

ACKNOWLEDGEMENTS

The test results of the cyclic undrained triaxial test on undisturbed weathered granite fill (locally called Masado) and alluvial clay were provided by Mr. Akihiko Uchida, Takenaka Corporation. The authors express their gratitude to him.

REFERENCES

1. Architectural Institute of Japan ”Recommendations for design of building foundations.” 2001 (in Japanese).
2. Iwasaki, T., Tatsuoka, F., Tokida, K. and Yasuda, S. ”A practical method for assessing soil liquefaction potential based on case studies at various sites in Japan.” Proceedings 2nd International Conference on Microzonation, San Francisco, Vol.2, pp. 885-896, 1978.
3. Kazama, M. ”Reconsideration of the shear stress ratio generated by earthquakes.” Tsuchi-to-Kiso, JSSMFE, Vo.47, No.8, Ser.No.499, pp. 13-16, 1999 (in Japanese).
4. Yamaguchi, A. ”Seismic behavior of Kobe's artificial islands during the 1995 Hyogo-ken Nambu Earthquake.” Doctor Thesis at Tohoku University, 2001 (in Japanese).
5. Igarashi, S. ”Energy-based factor of safety against liquefaction.” Proceedings of JSCE No.455/I-21, pp. 13-24, 1992.
6. Kazama, M. ”A new idea for evaluating liquefaction strength based on accumulative hysteretic energy.” Proceedings of the 32nd. Japan National Conference on JSSMFE., pp. 723-724, 1997 (in Japanese).
7. Akiyama, H. ”Earthquake-resistant design method for buildings based on energy balance.” Gihodo Press, 1999 (in Japanese).
8. Kusakabe, S. and Morio, S. ”The develop of a substructure on-line testing system for seismic response analysis of geotechnical system.” Soils and Foundations, Vol. 35, No.2, pp.117-125, 1995.
9. Adachi, T., Yamada, M., Sekihara, H. and Enami, A. ”Pseudo-dynamic test on intensity of earthquake ground motions at occurrence of liquefaction of subsurface layers.” Journal of Structural and Construction Engineering, Trnsactions of Architectural Institute of Japan, No.505, pp. 85-91, 1998 (in Japanese).
10. Inoue, Y., Osawa, Y., Matsushima, Y., Kitagawa, Y., Yamazaki, Y., and Kawamura, S. ”A Proposal for seismic design procedure of apartment houses including Soil-structure interaction effect.” Proceedings of 9th World Conference on Earthquake Engineering, Vol.VIII, Tokyo-Kyoto, pp. 365-370,1998.
11. Tanaka, Y., Kanatani, M., Hataya, R., Sato, K., Kawai, T. and Kudo, K. ”Evaluation of liquefaction potential of gravelly soil layer based on field performance data.” Proceedings of JSCE No.666/III-53, pp. 55-72, 2000 (in Japanese).
12. Kobe City Report ”Investigation of ground deformation of reclaimed ground due to Hyogo-ken Nanbu earthquake.” Port Island, Rokko Island, pp. 1-119, 1995 (in Japanese).
13. Hatanaka, M., Uchida, A. and Ohara, J. ”Liquefaction characteristics of a gravelly fill liquefied during the 1995 Hyogo-ken Nanbu earthquake.” Edition of Soils and Foundations, Vol.37, No.3, pp. 107-115, 1997.